HHS Public Access

Author manuscript

Ann Anat. Author manuscript; available in PMC 2017 March 01.

Published in final edited form as:

Ann Anat. 2016 March ; 204: 29–35. doi:10.1016/j.aanat.2015.10.004.

Intra- and inter-observer reliability of quantitative analysis of the infra-patellar fat pad and comparison between fat- and non-fat-suppressed imaging—Data from the osteoarthritis initiative

E. Steidle-Kloc[*], **W. Wirth**, **A. Ruhdorfer**, **T. Dannhauer**, and **F. Eckstein**

Paracelsus Medical University Salzburg & Nuremberg, Institute of Anatomy, Strubergasse 21, A-5020 Salzburg, Austria

Abstract

The infra-patellar fat pad (IPFP), as intra-articular adipose tissue represents a potential source of pro-inflammatory cytokines and its size has been suggested to be associated with osteoarthritis (OA) of the knee. This study examines inter- and intra-observer reliability of fat-suppressed (fs) and non-fat-suppressed (nfs) MR imaging for determination of IPFP morphological measurements as novel biomarkers.

The IPFP of nine right knees of healthy Osteoarthritis Initiative participants was segmented by five readers, using fs and nfs baseline sagittal MRIs. The intra-observer reliability was determined from baseline and 1-year follow-up images. All segmentations were quality controlled (QC) by an expert reader. Reliability was expressed as root mean square coefficient of variation (RMS CV%).

After QC, the inter-observer reliability for fs (nfs) imaging was 2.0% (1.1%) for IPFP volume, 2.1%/2.5% (1.6%/1.8%) for anterior/posterior surface areas, 1.8% (1.8%) for depth, and 2.1% (2.4%) for maximum sagittal area. The intra-observer reliability was 3.1% (5.0%) for volume, 2.3%/2.8% (2.5%/2.9%) for anterior/posterior surfaces, 1.9% (3.5%) for depth, and 3.3% (4.5%) for maximum sagittal area. IPFP volume from nfs images was systematically greater (+7.3%) than from fs images, but highly correlated ($r = 0.98$).

The results suggest that quantitative measurements of IPFP morphology can be performed with satisfactory reliability when expert QC is implemented. The IPFP is more clearly depicted in nfs images, and there is a small systematic off-set versus analysis from fs images. However, the high linear relationship between fs and nfs imaging suggests that fs images can be used to analyze IPFP morphology, when nfs images are not available.

Keywords

Infra-patellar fat pad; Hoffa fat pad; Magnetic resonance imaging; Osteoarthritis; Knee joint; Reliability; Morphology

[*]Corresponding author. Tel.: +43 662 2420 80408; fax: +43 662242080409. eva.steidle@pmu.ac.at (E. Steidle-Kloc).

Appendix A. Supplementary data

Supplementary data associated with this article can be found, in the online version, at http://dx.doi.org/10.1016/j.aanat.2015.10.004.

1. Introduction

Osteoarthritis (OA) of the knee represents the most common form of arthritis and causes chronic disability and pain, particularly in the elderly (Felson et al., 1997; Peat et al., 2001; Torres et al., 2006). The relationship between the body mass index (BMI), thigh muscle strength, and knee OA has been studied intensely, but mechanical factors have failed to fully explain the relationship between obesity and increased risk of OA (Aspden, 2011; Griffin and Guilak, 2008). Pro-inflammatory mediators secreted by adipocytes (adipokines, e.g. leptin, interleukin-6) have recently been shown to promote articular tissue degradation (Hui et al., 2012; Scotece et al., 2013; Stannus et al., 2015), especially in obesity-associated OA, and adipose tissue has hence been suggested to play an endocrine role in the pathophysiology of OA (Clockaerts et al., 2010; Griffin and Guilak, 2008; Griffin et al., 2012; Issa and Griffin, 2012).

The infra-patellar fat pad (IPFP, or “Hoffa’s fat pad”) represents a unique structure of intra-articular albeit extra-synovial adipose tissue, which is in close spatial vicinity to the synovium and has been shown to be a source of inflammation and intra-articular leptin secretion (Gierman et al., 2013; Hui et al., 2012; Issa and Griffin, 2012; Klein-Wieringa et al., 2011). IPFP morphological measurements have, therefore, gained recent interest in OA research as potential biomarkers for exploring healthy tissue physiology, structure-function relationships, disease status, and disease progression.

Based on 3D volumetric analysis of sagittal magnetic resonance images (MRI), a 41% greater IPFP volume has been reported in healthy men than in healthy women (Diepold et al., 2015). Even after normalizing IPFP volume to body weight, men still displayed a 9% greater ratio of IPFP volume/body weight than women. These findings were in contrast to a much greater proportion of subcutaneous fat (50%) of the thigh in women within the same study (Diepold et al., 2015). In knee OA patients, a larger IPFP maximum sagittal area has been reported to be associated with less knee pain and reduced risk of medial cartilage defects (Pan et al., 2014). In another study, a larger IPFP maximum area was reported to be negatively associated with radiographic OA and knee pain, suggesting a protective role for IPFP through a possible mechanism of mechanical shock absorption (Han et al., 2014). Somewhat in contrast to the above findings, a greater IPFP volume and its significant correlation with more severe knee pain was reported in subjects with symptomatic and radiographic patellofemoral OA, compared with asymptomatic controls without radiographic signs of OA (Cowan et al., 2015).

Given these emerging studies on IPFP morphological measurements as biomarkers, it is important to establish to what extent quantitative measurement of the IPFP from MRI is reliable (precise). Intuitively, non-fat-suppressed (nfs) MRIs appear most suitable for the purpose of measuring the IPFP, because these adipose tissues are displayed with high signal intensity and good contrast to neighboring non-adipose tissues, such as bone cortices, ligaments, menisci, and cartilage. However, many epidemiological studies preferentially acquire fat-suppressed (fs) knee MRIs, because they are better suited for evaluating structural pathology of articular tissues, such as menisci, cartilage and bone marrow (Guermazi et al., 2013), and it has not been previously shown whether these permit analysis

of the IPFP with similar reliability as in non-fs images. Therefore, the specific purpose of the current study has been to determine the inter-observer and intra-observer reliability (precision) of IPFP morphology, and to compare quantitative measurements of the IPFP obtained from intermediate-weighted fs versus nfs MRIs. These measurements included IPFP volume, surface areas, depth (mean thickness), maximum sagittal area (the slice with the greatest IPFP area), and central slice sagittal area (the middle slice of all segmented slices in each data set).

2. Material and methods

2.1. Study sample

The participants used in this analysis were taken from the healthy reference cohort of the Osteoarthritis Initiative (OAI) data base (Eckstein et al., 2014, 2012). The OAI is a multicenter, longitudinal, prospective observational study that provides public access to clinical datasets, radiographs, MRIs and bio-specimens from serum and urine, so that researchers can explore the predictive value of biomarkers for knee OA onset and progression (Eckstein et al., 2014, 2012). Between February 2004 and May 2006, the OAI recruited 4796 participants, aged 45–79 years, at four clinical centers. The participants were either part of a healthy reference cohort (n = 122, without risk factors for incident knee OA), were at risk of developing knee OA (i.e. incidence cohort), or had symptomatic knee OA at the time point of recruitment (i.e. progression cohort). The OAI protocol is consistent with the principles of the Declaration of Helsinki (World Medical Association) and is registered under clinicaltrials.gov (identifier: NCT00080171). The OAI received ethical approval by the Institutional Review Boards (IRB) at each of the four clinical sites, and all participants gave informed consent. This informed consent includes use of the publicly available images and clinical data that will be used in this study.

Participants in the OAI healthy reference cohort had to have no apparent radiographic signs of knee OA, no knee pain, and no risk factors of knee OA, including a normal body weight. The reliability of IPFP morphology in this study was assessed in nine right knees (5 women, 4 men) of the OAI healthy reference cohort. These were also selected to have axial MRI data of the thigh at baseline and 2-year follow-up; these thigh images were not relevant to the current study, but were previously used to report the inter- and intra-observer reliability of subcutaneous and intermuscular adipose tissue in the thigh (Dannhauer et al., 2015).

2.2. MR image acquisition

The MRI acquisition protocol of the OAI has been previously described in detail (Eckstein et al., 2012; Peterfy et al., 2008). All MRIs were acquired using 3 Tesla Magnetom Trio magnets (Siemens Healthcare Erlangen, Germany) and a quadrature knee coil. To segment and measure the IPFP, we used (a) the sagittal fat-suppressed (fs) intermediate-weighted turbo spin-echo sequence (IW TSE; time of repetition = 3200 ms; time of echo = 30 ms; slice thickness 3.0 mm; in plane resolution 0.36 mm × 0.36 mm; Fig. 1A and B) that was acquired in both knees of all OAI participants, and (b) the sagittal non-fat-suppressed (nfs) spin-echo MRI sequence (time of repetition = 2700 ms; time of echo = 30 ms; slice thickness 3.48 mm; in plane resolution 0.36 mm × 0.36 mm; Fig. 1C and D). The latter

imaging sequence was only acquired in the right knees of all OAI participants, as part of a multi-echo spin-echo (MESE) sequence used to evaluate cartilage composition by its transverse relaxation time (T2). The 30 ms time of echo acquisition of the MESE was selected in order to provide consistency in that parameter between the fs and nfs acquisition.

2.3. Image analysis

Manual segmentation of the knees was performed by one postdoc (E.S.) and four medical students (J.D., A.P., T.P. and F.H.) of the Paracelsus Medical University. These were initially trained using three test data sets that were not part of the current study. All five readers processed the fs images; three of them also performed segmentation of the nfs images.

During the segmentation process, the imaging parameters (brightness, intensity, contrast, gray value limit) were adjusted manually in each image. Each reader processed all slices that clearly depicted the IPFP. The anterior border of the IPFP (facing the lig. patellae) was segmented using one label (green marker) and the posterior border (the one facing the knee joint) using another label (magenta marker; Fig. 2).

A detailed description of the segmentation process has been provided previously in this journal (Diepold et al., 2015). All segmentations were quality controlled by a postdoc anatomist (A.R.) with ample experience in image analysis of musculoskeletal tissues. The IPFP volume, the anterior and posterior surface area, depth, maximum sagittal area and central slice area were computed using custom software.

No test–retest images with repositioning at one point in time were available from the OAI. To overcome this, and to additionally assess variability associated with change in measurement and biological conditions in healthy subjects, the intra-observer variability of the IPFP segmentation was evaluated by segmenting baseline and 1-year follow-up (Y1) acquisitions of the above nine knees by one reader (E.S.), using both fs and nfs images.

2.4. Statistics

All statistical analyses were performed using Microsoft Office Excel 2010, Microsoft Inc. Redmond, WA, USA) and StatView (1992–1998 SAS Inst. Inc. Cary, North Carolina, USA). Demographic data and quantitative measurements of IPFP morphology were reported as means and standard deviations (SDs).

The inter-observer and intra-observer reliability of the various quantitative measurements of the IPFP were described by the root mean square (RMS) coefficient of variation (CV) in percent (%) (Glüer et al., 1995). The RMS CV% expresses the magnitude of the variability of the measurement between the five readers (inter-observer reliability), or when different images are read by the same person (intra-observer reliability); larger values indicate greater variability (i.e. greater error) and consequently a lower degree of reliability or precision. To evaluate whether there were systematic differences between the readers, an ANOVA of repeated measurements was used. To evaluate whether there were systematic differences between baseline and 1-year follow-up (intra-observer test–retest), a paired *t*-test was applied.

Results from fs and nfs imaging were compared using ANOVA of repeated measurements. Further, the Pearson correlation coefficient was computed to evaluate whether results from both acquisition protocols were linearly related. To this end, the means of the three observers who had segmented both the fs and nfs images were used.

3. Results

The demographic data of the nine OAI healthy reference subjects are shown in Table 1. Although there was a slight longitudinal increase in body weight and BMI between baseline and 1-year follow-up, this difference did not reach statistical significance.

3.1. Inter-observer reliability of the IPFP using fat-suppressed imaging

Before expert QC, the inter-observer RMS CV% for IPFP volume from fs imaging was 11.7% across the nine data sets (Table 2). The mean volume (overall five readers) was 21.8 cm^3 and the difference between the readers ranged from −9.1% to 14.6%. After expert QC, the RMS CV% dropped to 2.0%, with a mean IPFP volume of 21.7 cm^3 and a difference in volume of −3.3% to 3.5% between the readers. Before QC, precision errors were observed to be larger for the IPFP anterior and posterior area than for IPFP volume, but smaller for IPFP depth, maximum sagittal area and central slice area. After expert QC, precision errors were similar for all quantitative IPFP measurements and were consistently smaller than before expert QC (Table 2). Before QC, the number of sagittal slices selected to segment IPFP morphology varied by up to four slices between the readers per data set, whereas after expert QC, the same number of slices was processed by each reader for each data set. Even after QC, ANOVA identified significant differences between readers in most measurements, except for IPFP depth ($p = 0.22$). However, quantitative measurements of the IPFP between the five readers showed a high linear relationship for all measurements ($r \geq 0.99$).

3.2. Inter-observer reliability of the IPFP using non-fat-suppressed imaging

Before QC, the inter-observer RMS CV% for IPFP volume from nfs imaging was 4.3% across the nine data sets (Table 2). The mean volume was 23.4 cm^3 and the difference in volume between the three readers ranged from −2.2% to 1.7%. After expert QC, the RMS CV% dropped to 1.1% with a mean IPFP volume of 23.8 cm^3 and a difference of −0.7% to 0.7% between the three readers. Before QC, precision errors were again observed to be larger for the IPFP anterior, posterior area than for IPFP volume, and were similar for IPFP depth, maximum and central slice sagittal area as for volume. After expert QC, precision errors were similar for all quantitative IPFP measurements and were consistently lower than before expert QC (Table 2). Before QC, the number of sagittal slices selected to segment IPFP morphology varied by only one slice between the three readers, whereas after expert QC, the same number of slices was processed by all readers for each data set. Even after QC, ANOVA identified significant differences between readers in most measurements, except for posterior surface ($p = 0.49$). However, as for fs imaging, volumetric results of the IPFP between the three observers showed a high linear correlation for all comparisons ($r \geq 0.99$).

3.3. Intra-observer reliability using fs and nfs imaging

Using fs imaging, the intra-observer RMS CV% for the IPFP volume was 7.0% before and 3.1% after expert QC (Table 3). There were no significant differences in IPFP measurements between baseline and 1-year follow-up, except for a reduction in maximum sagittal area (p = 0.02) and central slice area (p = 0.04). Using nfs imaging, the intra-observer RMS CV% for the IPFP volume was 7.2% before and 5.0% after expert QC; again there was no significant difference between baseline and 1-year follow-up, except for the reduction in maximum slice area (p = 0.03) and central slice area (p = 0.02; Table 3).

3.4. Comparison of IPFP morphology obtained from fs versus nfs imaging

Comparing results from fs with those from nfs imaging, ANOVA identified significant differences ($p < 0.05$) between both acquisition protocols for all quantitative measurements, when using mean values of the three readers for fs and nfs images. The mean differences were +1.6 cm^3 (95% CI 0.9, 2.3; +7.3%) between fs and nfs imaging-derived IPFP volume, +1.8 cm^2 (95% CI 1.1, 2.5; +11.0%) for the anterior area, +3.2 cm^2 (95% CI 2.0, 4.4; +10.6%) for the posterior area, −0.5 mm (95% CI −0.8, −0.1; −3.4%) for depth, +1.1 cm^2 (95% CI 1.0, 1.3; +15.9%) for maximum sagittal area, and +1.2 cm^2 (95% CI 1.0, 1.4; +15.7%) for central slice area.

However, results between both acquisition protocols displayed a high linear relationship, with Pearson correlation coefficients of 0.98 for IPFP volume, 0.93 for anterior surface, 0.92 for posterior surface, 0.87 for depth, 0.98 for maximum sagittal area, and 0.98 for central slice area (Fig. 3).

4. Discussion

Image-based IPFP morphological measurements potentially represent a novel biomarker in knee OA, and in the exploration of structure-function relationships of synovial joint tissues. Therefore, the current study has been performed to evaluate the inter- and intra-observer reliability of IPFP morphology, and to compare IPFP measurements derived from more commonly used fs than nfs MR images by relatively inexperienced (junior) researchers, who are commonly involved in studies requiring large scale segmentation.

We find that IPFP morphology can be reliably determined from both fs and nfs imaging, when expert QC is applied. Although there was a small, but statistically significant offset in the IPFP measurements between readers, the differences were relatively small, and much smaller than the inter-subject variability in IPFP measurements. Further, quantitative measurements between all readers were highly correlated. Not surprisingly, IPFP measurements were slightly greater when determined from nfs than from fs MRIs, but again values were highly correlated between both acquisition protocols.

The intra-observer analysis also revealed satisfactory reliability between baseline and 1-year follow-up. Although it may appear surprising that the intra-observer analysis showed greater variation than the inter-observer analysis, this is to be explained by the latter being performed on identical images, whereas intra-observer test–retest analysis relied on image acquisitions taken one year apart. The precision errors reported in the intra-observer analysis

thus also encompasses variability in imaging conditions and in biological conditions over this relatively long observation period, which, however, is relevant to longitudinal observational studies. In longitudinal studies in OA patients, IPFP size may be potentially influenced by variability in concomitant effusion. Future longitudinal studies on the effect of effusion on IPFP volume should thus take into account the normal variability observed here in healthy OAI participants over a one year period, in which effusion was unlikely due to the lack of risk factors of OA.

As previously recommended (Glüer et al., 1995), the RMS CV% was determined as a measure of reliability. Although a limitation of this study is the relatively small sample size of nine data sets, the degrees of freedom of the present inter-observer analysis is $9 \times (5 - 1) = 36$, which is above the minimum of 27 degrees of freedom recommended by Glüer et al. (1995), insuring that the real precision error is not underestimated by more than 30%. The inter-observer variability (RMS CV%) of quantitative measurements of thigh adipose tissue cross sectional areas from MRI was reported to be 2.2% for subcutaneous fat, and 14.7% for intermuscular fat (Dannhauer et al., 2015); that for medial meniscus volume was reported to be 5.4% (Siorpaes et al., 2012). The intra-observer variability of quantitative measurements of thigh adipose tissue was 10.7% for subcutaneous fat, and 12.4% for intermuscular fat (Dannhauer et al., 2015) with a 2-year interval in between data acquisition. For comparison, the intra-observer variability of the vastus medialis anatomical muscle cross-sectional areas was reported to be 4.3/4.5% (painful/painless knees), with a 1-year interval in between data analysis (Sattler et al., 2014), and the intra-observer reliability of cartilage thickness and volume measurements in the knee was reported to range from 2.1 to 3.3% (Eckstein et al., 2008). The reliability values reported here are thus in the range of previously reported precision errors of other musculoskeletal tissues, for which imaging biomarkers have been developed.

Before QC, the reliability errors for 3D volumes and anterior/posterior were higher than that of depth, maximum sagittal or central slice area, particularly in the fs images. This and our own observations suggest that the greatest source of inter-observer variability is segmentation uncertainty in peripheral (medial and lateral) regions of the IPFP, in particular in context of which slice to start and terminate IPFP segmentation. While the different parameters computed here are not independent and correlated to each other, future studies will have to show which of these have the highest sensitivity to change in longitudinal trials, and which approach is thus the most efficient in large-scale applications. As the central part of the IPFP is constrained by the clearly visible femoral and tibial bone, patella, lig. patellae and menisci, the medial and lateral IPFP periphery shows less clear borders with adjacent tissue. However, the periphery may be of particular relevance in studying IPFP volume variation between subjects and within subjects longitudinally, as this is where adipose tissue may be potentially added or removed with change in body weight or BMI. However, our results show that 3D measurements containing the full IPFP volume areas are as reliable as the analysis of a single sagittal MRI slice, when QC is performed and the number of slices to be processed is clearly defined by an expert reader. All readers were untrained in image analysis to start with, and were then trained on the same three test data sets. Given the limited initial experience of the readers, it is not surprising that a relatively large variability was observed before expert QC. This is most likely caused by different individual

perspectives of where the borders of the IPFP are located and may also be affected by partial volume effects in regions where the sagittal images are not fully perpendicular to the IPFP surfaces. Relatively inexperienced (junior) researchers participated in the study, as these are commonly involved in studies requiring large scale segmentation. It is quite possible that the inter-observer reliably before QC would have been higher, if experienced radiologists or more experienced imaging experts had been involved. Whether or not QC is paramount regardless of the experience of the readers will have to be shown in separate studies, but, for the time being, a rule-based approach that clearly defines the first/last slice of the IPFP, combined with expert QC, are recommended for providing reliability and consistent results between different readers.

The OAI data base provides fs MRIs for both knees, whereas nfs MRIs are only available for the right knees. If only nfs images could be used for the purpose of IPFP analysis, this would limit the number of possible questions and study designs, prohibiting between-knee, within person comparisons and any analysis that relies on left knees of interest in the OAI. The somewhat greater inter-observer reliability in nfs images before QC compared with fs imaging is likely caused by the higher contrast between IPFP borders and surrounding tissues, when MRI signal from the adipose tissue is not suppressed. Yet, after expert QC, the reliability of both acquisition protocols was in a similar range, and measurements obtained with either method were highly correlated. This is important, because the MR imaging protocols of many epidemiological studies are restricted to fs imaging, as these images are generally better suited for evaluating structural pathology of synovial joint tissues, such as menisci, cartilage or bone marrow (Guermazi et al., 2013). The possibility to determine IPFP morphological measurements in fs images with similar reliability as for nfs images therefore provides much wider opportunity for the use of these biomarkers in epidemiological and clinical studies.

IPFP imaging measurements as potential biomarkers may be of particular interest in clinical trials that explore non-pharmacological interventions in knee OA. It has recently been reported that IPFP volume may be responsive to exercise and/or diet as treatment of knee OA, with the combination of exercise and diet being most effective in reducing IPFP volume (Pogacnik Murillo et al., 2015) and in providing clinical improvement of knee OA (Messier et al., 2013). Further studies may be directed at exploring IPFP variation as a function of BMI (weight gain or weight loss), radiographic knee OA status, knee pain, and to what extent the IPFP may vary under these conditions. The implementation of a robust standard measurement procedure that permits results of different readers to be pooled would hence be of great interest in this field of research.

5. Conclusion

This is the first study to systematically explore the inter- and intra-observer reliability of quantitative 3D analysis of IPFP morphologic measurements from MRI, as novel biomarkers in knee OA. The results suggest that quantitative measurements of IPFP morphology can be performed with satisfactory reliability when expert QC is implemented. The IPFP is more clearly depicted in nfs images, and there is a small systematic off-set versus analysis from fs images. However, the high linear relationship between fs and nfs

imaging suggests that fs images can be used to analyze IPFP morphology, when nfs images are not available.

Supplementary Material

Refer to Web version on PubMed Central for supplementary material.

Acknowledgments

Funding

We would like to thank Aaron Pogacnik Murillo, Julian Diepold, Franziska Haniel und Tobias Peterson for participating as readers in this study. Further, we would like to thank the OAI participants, OAI investigators, OAI clinical staff, OAI coordinating center at the UCSF and the OAI funders for generating this publicly available data. The OAI is a public-private partnership comprised of five contracts (N01-AR-2-2258; N01-AR-2-2259; N01-AR-2-2260; N01-AR-2-2261; N01-AR-2-2262) funded by the National Institutes of Health. Funding partners include Merck Research Laboratories, Novartis Pharmaceuticals Corporation, GlaxoSmithKline, and Pfizer. Inc. Private Sector funding for the OAI is managed by the FNIH.

The image analysis performed in this study was supported by funds from the Paracelsus Medical University Research Fund (PMU FFF R-14/01/057-STD).

Abbreviations

3D	three dimensional
BMI	body mass index
fs	fat-suppressed
IPFP	infra-patellar fat pad
MRI	magnetic resonance images
nfs	non-fat-suppressed
OA	osteoarthritis
OAI	osteoarthritis initiative
QC	quality control
RMS CV%	root mean square coefficient of variation

References

Aspden RM. Obesity punches above its weight in osteoarthritis. Nat. Rev. Rheumatol. 2011; 7:65–68. [PubMed: 20717100]

Clockaerts S, Bastiaansen-Jenniskens YM, Runhaar J, Van Osch GJVM, Van Offel JF, Verhaar JAN, De Clerck LS, Somville J. The infrapatellar fat pad should be considered as an active osteoarthritic joint tissue: a narrative review. Osteoarthritis Cartilage. 2010; 18:876–882. [PubMed: 20417297]

Cowan SM, Hart HF, Warden SJ, Crossley KM. Infrapatellar fat pad volume is greater in individuals with patellofemoral joint osteoarthritis and associated with pain. Rheumatol. Int. 2015; 35:1439–1442. [PubMed: 25782586]

Dannhauer T, Ruhdorfer A, Wirth W, Eckstein F. Quantitative relationship of thigh adipose tissue with pain, radiographic status, and progression of knee osteoarthritis: longitudinal findings from the osteoarthritis initiative. Invest. Radiol. 2015; 50:268–274. [PubMed: 25419827]

Diepold J, Ruhdorfer A, Dannhauer T, Wirth W, Steidle E, Eckstein F. Sex-differences of the healthy infra-patellar (Hoffa) fat pad in relation to inter-muscular and subcutaneous fat content—data from the osteoarthritis initiative. Ann. Anat. 2015; 200C:30–36. [PubMed: 25723518]

Eckstein F, Buck RJ, Burstein D, Charles HC, Crim J, Hudelmaier M, Hunter DJ, Hutchins G, Jackson C, Kraus VB, Lane NE, Link TM, Majumdar LS, Mazzuca S, Prasad PV, Schnitzer TJ, Taljanovic MS, Vaz A, Wyman B, Le Graverand M-PH. Precision of 3.0 Tesla quantitative magnetic resonance imaging of cartilage morphology in a multicentre clinical trial. Ann. Rheum. Dis. 2008; 67:1683–1688. [PubMed: 18283054]

Eckstein F, Kwoh CK, Link TM. Imaging research results from the osteoarthritis initiative (OAI): a review and lessons learned 10 years after start of enrolment. Ann. Rheum. Dis. 2014; 73:1289–1300. [PubMed: 24728332]

Eckstein F, Wirth W, Nevitt MC. Recent advances in osteoarthritis imaging—the osteoarthritis initiative. Nat. Rev. Rheumatol. 2012; 8:622–630. [PubMed: 22782003]

Felson DT, Zhang Y, Hannan MT, Naimark A, Weissman B, Aliabadi P, Levy D. Risk factors for incident radiographic knee osteoarthritis in the elderly: the Framingham study. Arthritis Rheum. 1997; 40:728–733. [PubMed: 9125257]

Gierman LM, Wopereis S, van El B, Verheij ER, Werff-van der Vat BJC, Bastiaansen-Jenniskens YM, van Osch GJVM, Kloppenburg M, Stojanovic-Susulic V, Huizinga TWJ, Zuurmond A-M. Metabolic profiling reveals differences in concentrations of oxylipins and fatty acids secreted by the infra-patellar fat pad of donors with end-stage osteoarthritis and normal donors. Arthritis Rheum. 2013; 65:2606–2614. [PubMed: 23839996]

Glüer CC, Blake G, Lu Y, Blunt BA, Jergas M, Genant HK. Accurate assessment of precision errors: how to measure the reproducibility of bone densitometry techniques. Osteoporos. Int. 1995; 5:262–270. [PubMed: 7492865]

Griffin TM, Guilak F. Why is obesity associated with osteoarthritis? Insights from mouse models of obesity. Biorheology. 2008; 45:387–398. [PubMed: 18836239]

Griffin TM, Huebner JL, Kraus VB, Yan Z, Guilak F. Induction of osteoarthritis and metabolic inflammation by a very high-fat diet in mice: effects of short-term exercise. Arthritis Rheum. 2012; 64:443–453. [PubMed: 21953366]

Guermazi A, Roemer FW, Haugen IK, Crema MD, Hayashi D. MRI-based semiquantitative scoring of joint pathology in osteoarthritis. Nat. Rev. Rheumatol. 2013; 9:236–251. [PubMed: 23321609]

Han W, Cai S, Liu Z, Jin X, Wang X, Antony B, Cao Y, Aitken D, Cicuttini F, Jones G, Ding C. Infrapatellar fat pad in the knee: is local fat good or bad for knee osteoarthritis? Arthritis Res. Ther. 2014; 16:R145. [PubMed: 25008048]

Hui W, Litherland GJ, Elias MS, Kitson GI, Cawston TE, Rowan AD, Young DA. Leptin produced by joint white adipose tissue induces cartilage degradation via upregulation and activation of matrix metalloproteinases. Ann. Rheum. Dis. 2012; 71:455–462. [PubMed: 22072016]

Issa RI, Griffin TM. Pathobiology of obesity and osteoarthritis: integrating biomechanics and inflammation. Pathobiol. Aging Age Relat. Dis. 2012; 9:2.

Klein-Wieringa IR, Kloppenburg M, Bastiaansen-Jenniskens YM, Yusuf E, Kwekkeboom JC, El-Bannoudi H, Nelissen RGHH, Zuurmond A, Stojanovic-Susulic V, Van Osch GJVM, Toes REM, Ioan-Facsinay A. The infrapatellar fat pad of patients with osteoarthritis has an inflammatory phenotype. Ann. Rheum. Dis. 2011; 70:851–857. [PubMed: 21242232]

Messier SP, Mihalko SL, Legault C, Miller GD, Nicklas BJ, DeVita P, Beavers DP, Hunter DJ, Lyles MF, Eckstein F, Williamson JD, Carr JJ, Guermazi A, Loeser RF. Effects of intensive diet and exercise on knee joint loads, inflammation, and clinical outcomes among overweight and obese adults with knee osteoarthritis: the IDEA randomized clinical trial. JAMA. 2013; 310:1263–1273. [PubMed: 24065013]

Pan F, Han W, Wang X, Liu Z, Jin X, Antony B, Cicuttini F, Jones G, Ding C. A longitudinal study of the association between infrapatellar fat pad maximal area and changes in knee symptoms and structure in older adults. Ann. Rheum. Dis. 2014; 74:1818–1824. [PubMed: 24833783]

Peat G, McCarney R, Croft P. Knee pain and osteoarthritis in older adults: a review of community burden and current use of primary health care. Ann. Rheum. Dis. 2001; 60:91–97. [PubMed: 11156538]

Peterfy CG, Schneider E, Nevitt M. The osteoarthritis initiative: report on the design rationale for the magnetic resonance imaging protocol for the knee. Osteoarthritis Cartilage. 2008; 16:1433–1441. [PubMed: 18786841]

Pogacnik Murillo AL, Wirth W, Beavers D, Loeser RF, Nicklas BJ, Hunter D, Eckstein F, Messier SP. Impact of diet and/or exercise intervention on infra-patellar fat pad morphology—data from the intensive diet and exercise for arthritis (IDEA) trial. Osteoarthritis Cartilage. 2015; 23(Suppl.):A389–A390.

Sattler M, Dannhauer T, Ring-Dimitriou S, Sänger AM, Wirth W, Hudelmaier M, Eckstein F. Relative distribution of quadriceps head anatomical cross-sectional areas and volumes—sensitivity to pain and to training intervention. Ann. Anat. 2014; 196:464–470. [PubMed: 25153247]

Scotece M, Conde J, Lopez V, Lago F, Pino J, Gomez-Reino JJ, Gualillo O. Leptin in joint and bone diseases: new insights. Curr. Med. Chem. 2013; 20:3416–3425. [PubMed: 23746275]

Siorpaes K, Wenger A, Bloecker K, Wirth W, Hudelmaier M, Eckstein F. Interobserver reproducibility of quantitative meniscus analysis using coronal multiplanar DESS and IWTSE MR imaging. Magn. Reson. 2012; 67:1419–1426.

Stannus OP, Cao Y, Antony B, Blizzard L, Cicuttini F, Jones G, Ding C. Cross-sectional and longitudinal associations between circulating leptin and knee cartilage thickness in older adults. Ann. Rheum. Dis. 2015; 74:82–88. [PubMed: 24078677]

Torres L, Dunlop DD, Peterfy C, Guermazi A, Prasad P, Hayes KW, Song J, Cahue S, Chang A, Marshall M, Sharma L. The relationship between specific tissue lesions and pain severity in persons with knee osteoarthritis. Osteoarthritis Cartilage. 2006; 14:1033–1040. [PubMed: 16713310]

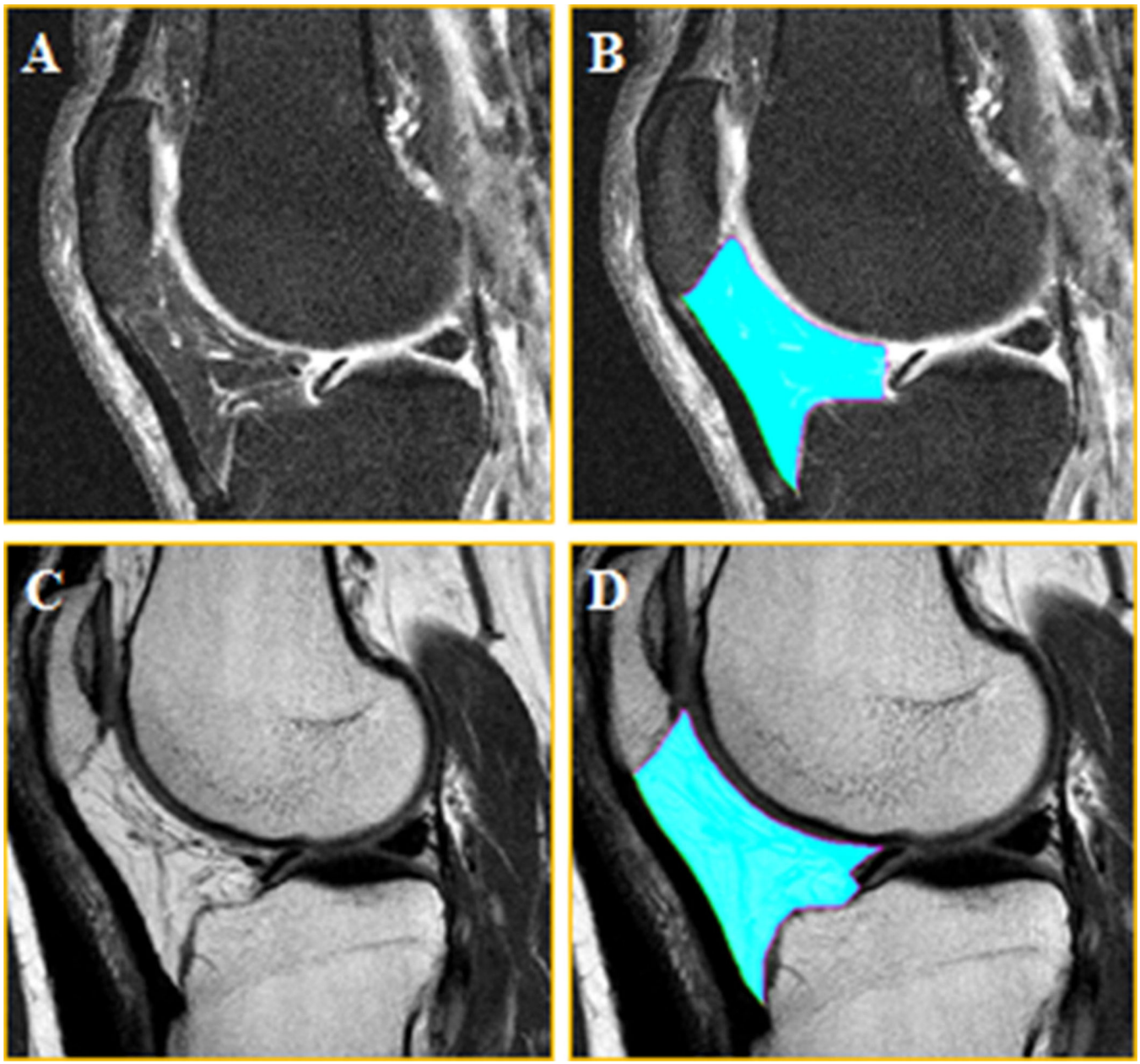

Fig. 1. Intermediate-weighted fat-suppressed and non-fat-suppressed sagittal MR images of the infra-patellar fat pad (IPFP)

(A) Fat-suppressed image without segmentation of the IPFP (B) Fat-suppressed image with segmentation of the IPFP (C) Non-fat-suppressed image without segmentation of the IPFP (D) Non-fat-suppressed image with segmentation of the IPFP

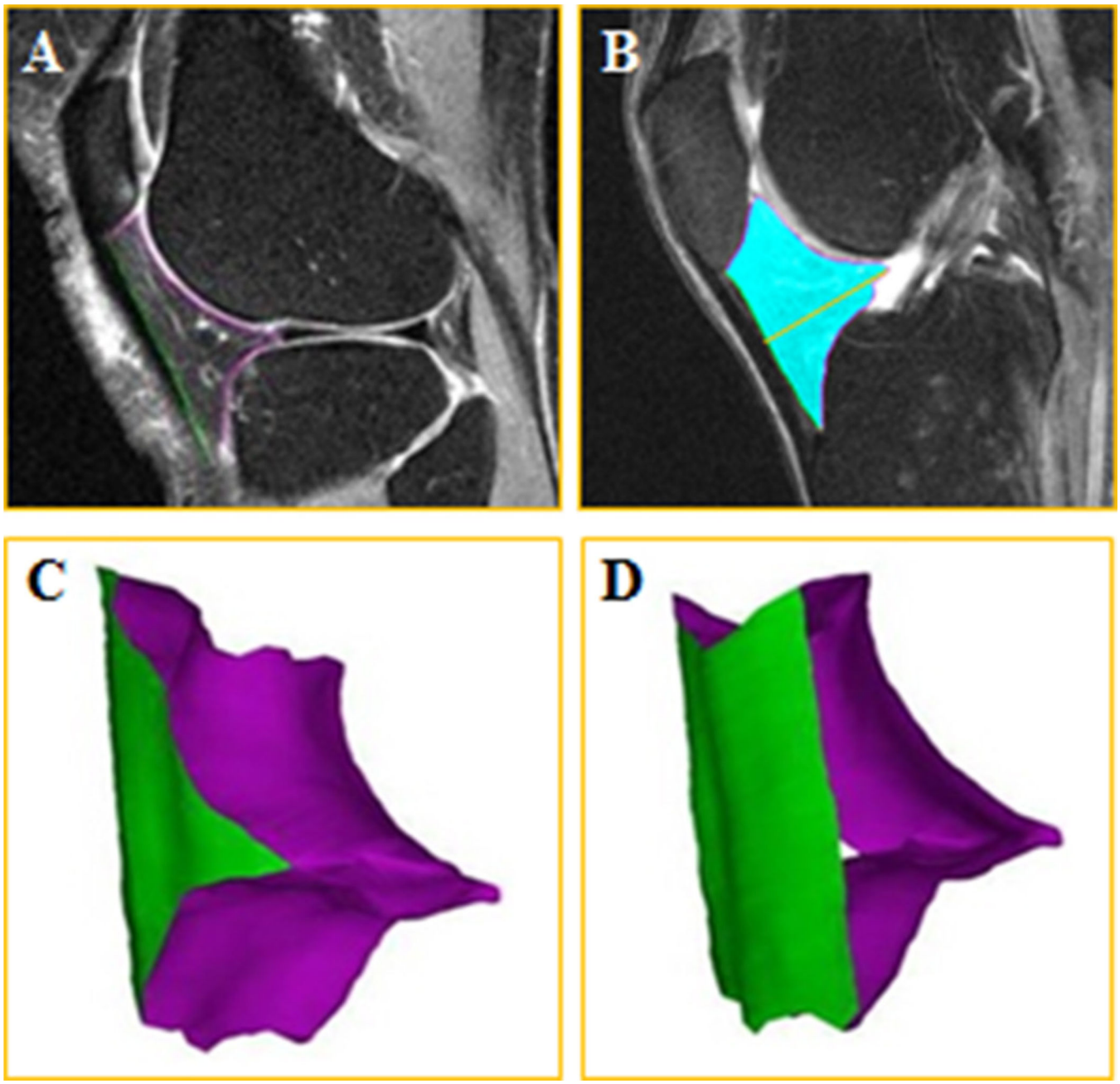

Fig. 2. Illustration of the infra-patellar fat pad segmentation and 3D reconstruction

(A) Sagittal fat-suppressed MRI of the knee joint showing segmentation of the anterior surface (green label), and posterior surface (magenta label) of the IPFP, (B) IPFP volume (blue) and depth (orange line), (C) 3D reconstruction of the IPFP viewed from posterior-lateral and (D) from anterior-lateral. (For interpretation of the references to color in this figure legend, the reader is referred to the web version of this article.)

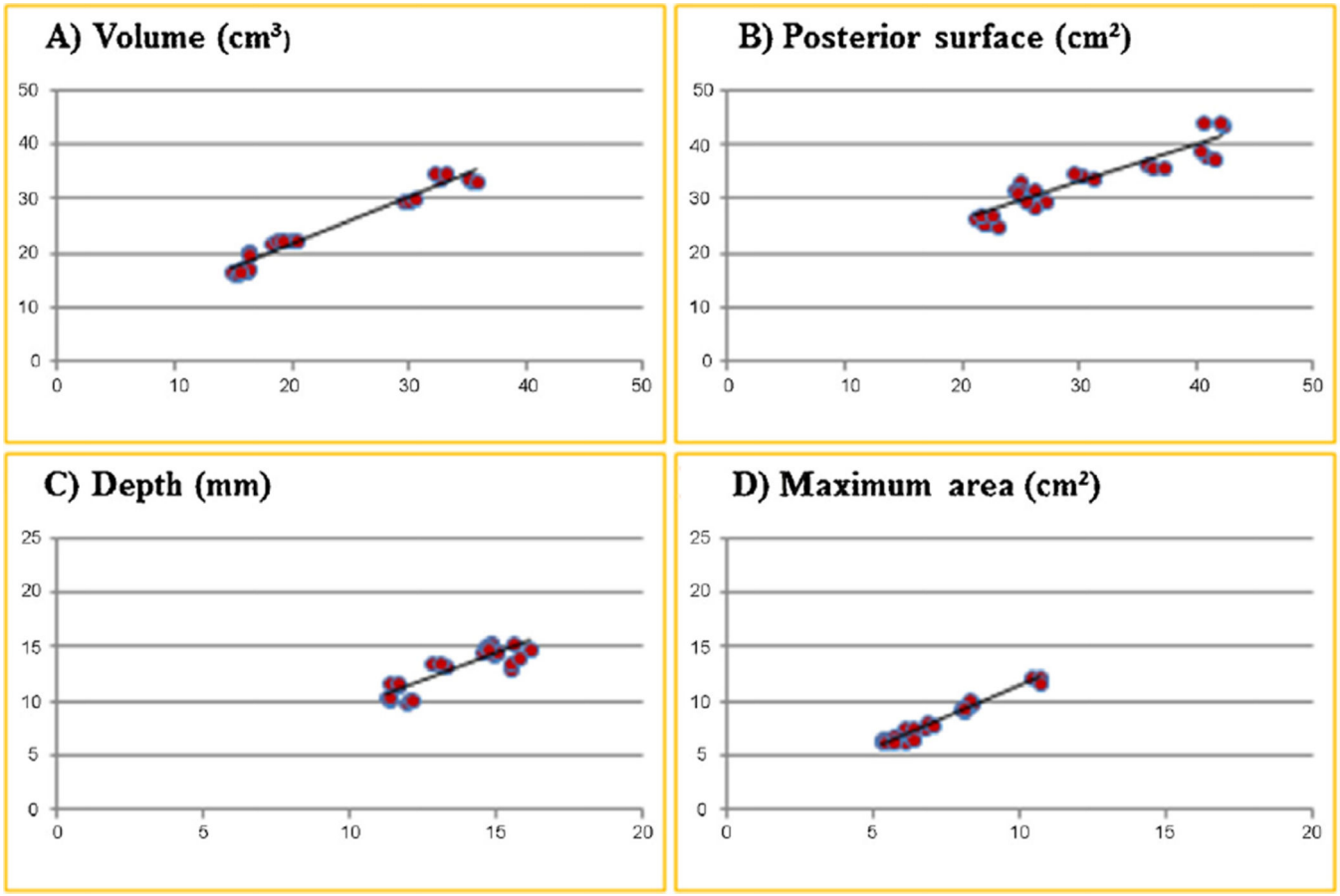

Fig. 3. Linear relationship of infra-patellar fat pad (IPFP) fat-suppressed and non-fat-suppressed MRIs

Linear relationship between fat suppressed TSE (*x*-axis) and non-fat suppressed MESE (*y*-axis) sequence for the infra-patellar fat pad (A) volume, (B) posterior surface, (C) depth and (D) maximum sagittal area; *Abbreviations:* MESE, multi-echo spin-echo sequence; TSE, turbo spin-echo sequence.

Table 1

Demographic data of the nine healthy participants of the OAI reference cohort examined in the current study.

	Baseline mean ± SD	Y1 mean ± SD	Absolute difference between BL and Y1	% Difference between BL and Y1	*p*-Value (*t*-test) between BL and Y1
Sex (f/m)	5/4				
Age (years)	54 ± 9 (46 to 77)				
Body height (cm)	165 ± 9				
Body weight (kg)	67 ± 14	70 ± 13	2.3	3.4	0.17
BMI (kg/m^2)	24 ± 3	25 ± 3	0.8	3.6	0.19

Abbreviations: BL, baseline; BMI, body mass index; Y1, year 1 follow-up; SD, standard deviation;

Ann Anat. Author manuscript; available in PMC 2017 March 01.

Table 2

Inter-observer variability of quantitative measures of the infra-patellar fat pad (IPFP) in healthy knees based on fat-suppressed (fs) and non-fat-suppressed (nfs) MRI data.

Inter-observer fat-suppressed (n = 9; after QC)	IPFP volume (cm^3)	IPFP anterior surface (cm^2)	IPFP posterior surface (cm^2)	IPFP depth (mm)	IPFP maximum sagittal area (cm^2)	IPFP central slice area (cm^2)
Observer 1	22.0 ± 8.1	15.8 ± 4.8	29.8 ± 7.9	13.8 ± 1.8	6.9 ± 1.6	6.7 ± 1.7
Observer 2	22.0 ± 8.1	16.1 ± 4.7	29.5 ± 7.5	13.5 ± 1.7	7.0 ± 1.8	6.8 ± 1.8
Observer 3	22.5 ± 8.2	16.2 ± 4.9	30.4 ± 7.8	13.8 ± 1.7	7.0 ± 1.7	6.9 ± 1.7
Observer 4	21.0 ± 7.6	15.3 ± 4.8	28.3 ± 7.0	13.6 ± 1.5	7.0 ± 1.6	6.7 ± 1.5
Observer 5	21.1 ± 7.2	15.2 ± 4.7	28.2 ± 7.0	13.9 ± 1.6	7.0 ± 1.7	6.7 ± 1.5
RMS CV% before QC	**11.7**	**14.3**	**14.3**	**4.4**	**3.5**	**5.5**
RMS CV% after QC	**2.0**	**2.1**	**2.5**	**1.8**	**2.1**	**2.4**
Inter-observer non-fat-suppressed (n = 9; after QC)	IPFP volume (cm^3)	IPFP anterior surface (cm^2)	IPFP posterior surface (cm^2)	IPFP depth (mm)	IPFP maximum sagittal area (cm^2)	IPFP central slice area (cm^2)
Observer 1	23.6 ± 7.0	17.9 ± 3.5	33.1 ± 5.8	13.0 ± 1.9	8.0 ± 2.0	7.9 ± 2.0
Observer 2	23.9 ± 7.2	17.7 ± 3.5	33.2 ± 6.0	13.4 ± 2.0	8.2 ± 1.9	8.1 ± 1.9
Observer 3	23.8 ± 7.2	17.7 ± 3.7	32.9 ± 5.7	13.3 ± 2.0	8.1 ± 1.9	8.0 ± 1.9
RMS CV% before QC	**4.3**	**6.6**	**4.9**	**3.7**	**3.8**	**4.4**
RMS CV% after QC	**1.1**	**1.6**	**1.8**	**1.8**	**2.4**	**2.4**

Values are reported as mean ± standard deviation (SD) after quality control (QC) by an expert reader.

Abbreviations: IPFP, infra-patellar fat pad; QC = quality control by an expert reader; RMS CV% = root mean square coefficient of variation.

Ann Anat. Author manuscript; available in PMC 2017 March 01.

Table 3

Intra-observer variability of quantitative measures of the infra-patellar fat pad (IPFP) in healthy knees based on fat-suppressed (fs) and non-fat-suppressed (nfs) MRI data.

Intra-observer fat-suppressed (n = 9)	IPFP volume (cm^3)	IPFP anterior surface (cm^2)	IPFP posterior surface (cm^2)	IPFP depth (mm)	IPFP maximum sagittal area (cm^2)	IPFP central slice area (cm^2)
BL	22.0 ± 8.1	16.1 ± 4.7	29.5 ± 7.5	13.5 ± 1.7	7.0 ± 1.8	6.8 ± 1.8
Y1	21.9 ± 8.3	16.1 ± 4.8	29.5 ± 8.0	13.5 ± 1.8	6.7 ± 1.7	6.6 ± 1.7
Mean difference (diff. %)	−0.1 (−0.2%)	±0.0 (−0.3%)	±0.0 (0.1%)	±0.0 (±0.0%)	−0.2 (−3.1%)	−0.2 (−3.0%)
95% CI	−0.6,0.5	−0.4,0.3	−0.6,0.7	−0.2,0.2	−0.4. −0.1	−0.4, −0.0
p-Value	0.87	0.80	0.91	0.99	0.02*	0.04*
RMS CV% before QC	**7.0**	**10.0**	**6.2**	**5.5**	**3.9**	**4.8**
RMS CV% after QC	**3.1**	**2.3**	**2.8**	**1.9**	**3.3**	**3.9**
Intra-observer non-fat-suppressed (n = 9)	IPFP volume (cm^3)	IPFP anterior surface (cm^2)	IPFP posterior surface (cm^2)	IPFP depth (mm)	IPFP maximum sagittal area (cm^2)	IPFP central slice area (cm^2)
BL	23.9 ± 7.2	17.7 ± 3.5	33.2 ± 6.0	13.4 ± 2.0	8.2 ± 1.9	8.1 ± 1.9
Y1	23.0 ± 6.6	17.5 ± 3.9	32.6 ± 5.5	13.1 ± 1.7	7.8 ± 1.8	7.6 ± 1.7
Mean difference (diff. %)	−0.9 (−3.8%)	−0.2 (−1.3%)	−0.6 (−1.9%)	−0.3 (−2.1%)	−0.4 (−4.3%)	−0.5 (−5.6%)
95% CI	−1.9,0.1	−0.6,0.1	−1.5,0.2	−0.7,0.1	−0.6, −0.1	−0.8, −0.2
p-Value	0.11	0.25	0.19	0.23	0.03*	0.02*
RMS CV% before QC	**7.2**	**8.7**	**6.1**	**4.9**	**6.0**	**6.2**
RMS CV% after QC	**5.0**	**2.5**	**2.9**	**3.5**	**4.5**	**5.9**

Values are reported as mean ± standard deviation (SD) after quality control (QC) by an expert reader.

Abbreviations: 95% CI, confidence interval; BL, baseline; RMS CV%, root mean square (RMS) coefficient of variation (CV%); Y1, year 1 follow-up.

* $p < 0.05$ is considered to be statistically significant.